Silicate Glass and Mineral Dissolution: Calculated Reaction Paths and Activation Energies for Hydrolysis of a Q^3 Si by H_3O^+ Using Ab Initio Methods

Louise J. Criscenti,*,†,‡ James D. Kubicki,† and Susan L. Brantley†

Department of Geosciences, The Pennsylvania State University, University Park, Pennsylvania 16802, and Geochemistry Department, Sandia National Laboratories, Albuquerque, New Mexico 87185

Received: December 10, 2004; In Final Form: September 26, 2005

Molecular orbital energy minimizations were performed with the B3LYP/6-31G(d) method on a $[((OH)_3SiO)_3SiOH-(H_3O^+)\cdot 4(H_2O)]$ cluster to follow the reaction path for hydrolysis of an Si−O−Si linkage via proton catalysis in a partially solvated system. The Q^3 molecule was chosen (rather than Q^2 or Q^1) to estimate the maximum activation energy for a fully relaxed cluster representing the surface of an Al-depleted acid-etched alkali feldspar. Water molecules were included in the cluster to investigate the influence of explicit solvation on proton-transfer reactions and on the energy associated with hydroxylating the bridging oxygen atom (O_{br}). Single-point energy calculations were performed with the B3LYP/6-311+G(d,p) method. Proton transfer from the hydronium cation to an O_{br} requires sufficient energy to suggest that the Si−(OH)−Si species will occur only in trace quantities on a silica surface. Protonation of the O_{br} lengthens the Si−O_{br} bond and allows for the formation of a pentacoordinate Si intermediate ($^{[5]}$Si). The energy required to form this species is the dominant component of the activation energy barrier to hydrolysis. After formation of the pentacoordinate intermediate, hydrolysis occurs via breaking the $^{[5]}$Si−(OH)−Si linkage with a minimal activation energy barrier. A concerted mechanism involving stretching of the $^{[5]}$Si−(OH) bond, proton transfer from the Si−$(OH_2)^+$ back to form H_3O^+, and a reversion of $^{[5]}$Si to tetrahedral coordination was predicted. The activation energy for Q^3Si hydrolysis calculated here was found to be less than that reported for Q^3Si using a constrained cluster in the literature but significantly greater than the measured activation energies for the hydrolysis of Si−O_{br} bonds in silicate minerals. These results suggest that the rate-limiting step in silicate dissolution is not the hydrolysis of Q^3Si−Obr bonds but rather the breakage of Q^2 or Q^1Si−O_{br} bonds.

Introduction

The rate-limiting step for dissolution of silicates and many aluminosilicates is thought to be the hydrolysis of Si−O−Si linkages (see White and Brantley[1] for a review). The rates of silicate dissolution are a function of the polymerization state of the Si cations.[2] The polymerization state is the average number of bridging oxygen atoms per tetrahedron (i.e., the $Q^{\#}$ of a Si^{4+} atom[3]), also known as the connectedness.[4] Silicate anions detected by ^{29}Si NMR spectroscopy in aqueous alkaline silicate solutions typically have Q^0, Q^1, Q^2, or Q^3 centers.[5−10] Silicate minerals are characterized by the degree of connectedness between one silicon atom and another. Figure 1 summarizes the measured dissolution rates for silicates as a function of connectedness. For example, the dissolution rate for a fully polymerized structure, such as quartz, is slower than that for a depolymerized chain structure such as wollastonite,[28] even though the rate-limiting step in each case may be hydrolysis of Si−O−Si linkages.

While connectedness appears to have a first-order control on dissolution rates, the nature of the charge-balancing cation has a second-order effect on the rate of dissolution, as shown for orthosilicates[30] and inosilicates.[20] The nature of nonframework cations also influences Si−O−Si bond lengths and angles. Smaller-scale experimental observations and molecular orbital calculations demonstrate that an increase in the coordination of a bridging oxygen either by protonation or by association with nonframework cations results in a small decrease in the Si−O bond length and a decrease in both the flexibility and the size of the Si−O−Si angles in silica tetrahedra.[30,31] These factors (along with experimental error) probably account for the spread in dissolution rates presented in Figure 1 for each connectedness value. In silicate glasses, silanol (SiOH) groups may promote the hydrolysis of adjacent Si−O−Si linkages because they are more hydrophilic than bridging oxygen atoms (O_{br}).

The preferential hydrolysis of Si tetrahedra with fewer linkages to other tetrahedra could lead to the dissolution of a silicate framework via specific sites found on cleavage planes (e.g., Q^3Si, Q^2Si), corners (Q^1Si), or edges (Q^2Si).[2] Gratz and Bird[32,33] measured face-specific dissolution rates and constructed dissolution-rate models to describe the dissolution of distinct crystal faces of quartz (SiO_2). The basal face consists entirely of Q^2Si; the major rhombohedron consists entirely of Q^3Si; and the prism face consists of repeating pairs of Q^2Si and Q^3Si layers. Their results suggest that a small but detectable difference in the activation energies of dissolution exists for different quartz faces and that this difference is due to different densities of the same type of reactive site on these faces.[32,33]

In this study, we begin to investigate the nature of this difference in hydrolysis as a function of polymerization by using ab initio methods to calculate the reaction path and activation energies for the acid hydrolysis of a Q^3Si model cluster. Abundant experimental evidence for increased rates of dissolu-

* Corresponding author. E-mail: ljcrisc@sandia.gov.
† The Pennsylvania State University.
‡ Sandia National Laboratories.

10.1021/jp044360a CCC: $33.50
Published on Web 12/07/2005

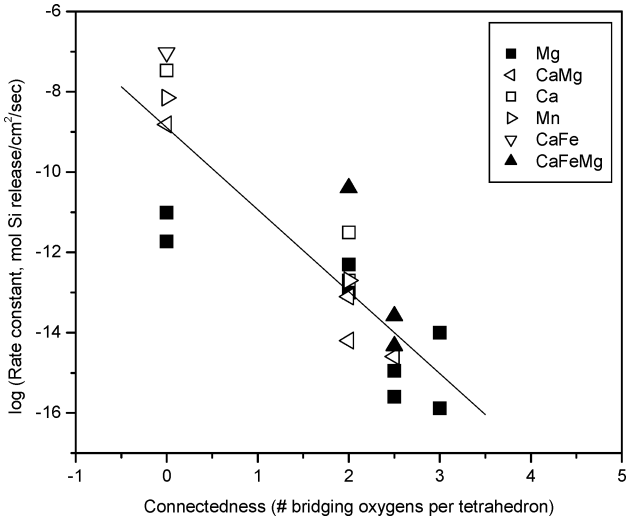

Figure 1. Measured dissolution rates for (Mg, Ca, Mn, Fe)-containing silicates as a function of connectedness or average number of bridging oxygens per tetrahedrally coordinated atom. A connectedness of 0 reflects an orthosilicate (Mg = forsterite[11,12] CaMg = monticellite,[13] CaFe = kirschsteinite,[13] Ca = calcium-olivine,[13] and Mn = tephroite[14]), 2 reflects a pyroxene (CaMg = diopside,[15] Mg = enstatite,[16,17] Ca = wollastonite,[18,19] Mn = rhodonite,[20] and CaFeMg = augite[21,22]), 2.5 reflects an amphibole (Mg = anthophyllite,[23,24] CaMg = tremolite,[25] and CaFeMg = hornblende,[26] with the addition of unpublished data from Brantley), and 3 reflects a phyllosilicate (Mg = talc, chrysotile). Compilations of data and figure are modeled after Brantley.[27]

tion in low pH solutions attributed to reaction with H_3O^+ below the point of zero charge have been reported for framework silicates,[34−44] quartz,[45,46] and other silicates. A recent summary of these data and macroscopic dissolution rate equations is provided in Brantley.[27] By evaluating relative activation energies for the dissolution of different silicate species through molecular orbital calculations, we plan to assess their relative rates of dissolution and establish the reaction mechanisms that dominate measured macroscopic dissolutions rates.

Comparison to Previous Molecular Modeling Studies. We begin by comparing our approach to previous studies using ab initio molecular orbital calculations to investigate the atomic processes of silicate hydrolysis. A number of papers has been published examining hydrolysis of silicate surfaces.[47−50] Three are of particular interest here because we focus on hydrolysis leading to dissolution rather than surface hydration/dehydration reactions. In the first study, Xiao and Lasaga[51] compared the hydrolysis of Si−O−Si and Si−O−Al bonds by either H_2O or H_3O^+. The molecular clusters used in the majority of their calculations were a disiloxane cluster H_6Si_2O and an equivalent aluminosilicate cluster H_6SiOAl. Si and Al in these clusters were Q^1 in nature. The dangling bonds of Si or Al were saturated with H atoms. The disiloxane cluster is illustrated in Figure 2A.

The hydrolysis of silica by H_3O^+ is believed to involve several elementary steps including the following: (1) adsorption of H_3O^+ to a bridging oxygen atom (defined by Xiao and Lasaga[51] as the protonation of the bridging oxygen atom and consequent release of H_2O), (2) formation of a pentacoodinate Si intermediate, and (3) cleavage of an $Si-O_{br}$ bond. For the study of H_3O^+ adsorption onto a silica surface, Xiao and Lasaga[51] wrote the following equation:

$$H_2O\cdots H_3O^+ + H_6Si_2O \leftrightarrow H_6Si_2O\cdots H_3O^+ + H_2O \quad (1)$$

This equation shows that the energy gained in adsorbing the

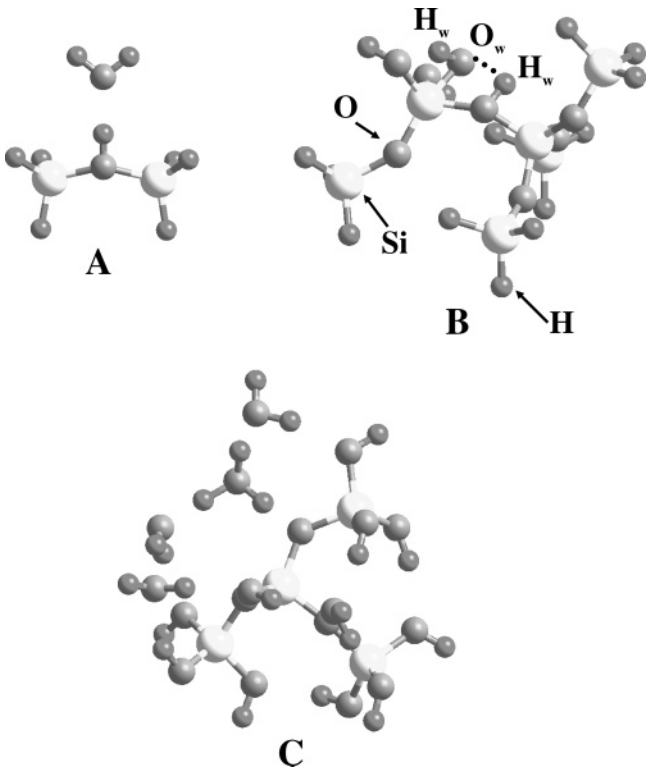

Figure 2. Comparison to previous molecular modeling studies. (A) Xiao and Lasaga,[51] (B) Pelmenschikov et al.,[56] and (C) this paper.

hydronium ion must be weighed against the energy lost in breaking a H-bond between this ion and a water molecule. Using MP2/6-31G(d), the $\Delta H°$ calculated by Xiao and Lasaga[51] for the reaction

$$H_3O^+ + H_2O \leftrightarrow H_3O^+\cdots H_2O \quad (2)$$

was 161 kJ/mol, in reasonable agreement with the experimental value of 151 kJ/ mol.[52] The calculated energy for the adsorption of a hydronium ion onto disiloxane or the enthalpy change for eq 1 was negative (i.e., $\Delta H° = -16$ kJ/mol). These calculations predict the favorable adsorption of H_3O^+ (or protonation of the bridging oxygen) on the silica surface.

Xiao and Lasaga[51] defined the activation energy for the hydrolysis of disiloxane under H_3O^+ catalysis as the energy required to cleave the $Si-O_{br}$ bond after protonation of the bridging oxygen atom because adsorption of H^+ at the O_{br} site was predicted to be thermodynamically favorable. The reactant cluster (Figure 2A) consisted of a protonated disiloxane and a water molecule that approached a Si atom to form a new Si−O bond while the original $Si-O_{br}$ cleaved. The activation enthalpy, $\Delta H°$, calculated using MP2/6-31G(d) was 100 kJ/mol. The reaction mechanism entailed the transient formation of a 5-coordinate Si atom as a bond formed between Si and the oxygen atom of the incoming H_2O. The predicted activation energy was reasonably close to experimental values for dissolution of silica that falls in a range between 60 and 95 kJ/mol.[41,53−55]

In other studies of silica hydrolysis using ab initio molecular orbital calculations, Pelmenschikov et al.[56,57] examined the effects of lattice resistance on $Si-O_{br}$ hydrolysis by a single water molecule. The model clusters used were based on the structure of the (001) and (111) planes of β-cristobalite. They were $Q^2Si-O-Q^4Si$ $[(H_3SiO)_3SiO-Si(OH)_2(OSiH_3)]$ (see Figure 2B) and $Q^3Si-O-Q^4Si$ $[(H_3SiO)_3SiOSi(OH)(OSiH_3)_2]$, each with an associated water molecule and each with the border Si

atoms saturated by H atoms. The positions of the border SiH_3 groups were fixed to model the structural constraints imposed by the β-cristobalite lattice (note: atoms in the crystal structure beyond this cluster were not included.) Cleavage of the Q^2Si-O_{br} and Q^3Si-O_{br} linkages was modeled. For comparison, Pelmenschikov et al.[56] also simulated cleavage of the Q^4Si-O_{br} bond in a constrained $Q^3Si-O-Q^4Si$ model cluster and cleavage of a Q^1Si-O_{br} bond in a completely relaxed $(HO)_3Si-O-Si(OH)_3$ cluster. The activation energies calculated using B3LYP/6-31G(d) were 71, 92, 138, and 205 kJ/mol for Q^1Si, Q^2Si, Q^3Si, and Q^4Si, respectively. Clearly, these results suggest that the hydrolysis rate may be a function of the Si polymerization state (i.e., Q#).

Pelmenschikov et al.[57] extended this study by performing additional calculations using B3LYP/6-31G(d) and a self-consistent isodensity polarized continuum model (SCIPCM) to include the long-range effects of solvation by bulk liquid water. They tested the hypothesis that the rate of silica dissolution is controlled by the hydrolysis of the first Si−O−Si bond of a Si surface species. The energy barrier calculated for the hydrolysis of a Q^2Si atom of β-cristobalite (121 kJ/mol) was higher by at least 29 kJ/mol than reported activation energies for the dissolution of silica (67−92 kJ/ mol)[45,51,58−60]at the point of zero net proton charge of the surface (PZPC). Therefore, Pelmenschikov et al.[57] proposed that dehydroxylation of the Si−OH HO−Si surface defect, or self-healing, occurs equally rapidly. The measured activation energy is then associated with the hydrolysis of the last Si−O−Si bond of the Si atoms (Q^1). The hydrolysis of this last bond is not hindered by the lattice resistance and leads to a theoretical activation energy (84 kJ/mol) that is in good agreement with experimental results. The inclusion of the solvent increased the activation energy by ≈16 kJ/mol, contributing to a higher activation energy than calculated in Pelmenschikov's previous work.[56]

This Paper. The silicate cluster used in this study consisted of a Q^3Si surrounded by three Q^1Si tetrahedra, one hydronium ion (H_3O^+), and four H_2O molecules (Figure 2C). The hydronium ion (H_3O^+) was used to hydrolyze the O_{br} between the Q^3Si and a Q^1Si. Two H_2O molecules were used to solvate the hydronium ion, and two were used to solvate the surface SiOH group. The formula for this cluster is $((OH)_3SiO)_3SiOH\cdot H_3O^+\cdot 4(H_2O)$. This cluster is positively charged and represents the exposure of a Q^3Si on a silica surface in an acidic solution. Like that of Xiao and Lasaga,[51] our cluster is used to investigate the reaction path and activation energy for the hydrolysis of an $Si-O_{br}$ bond under very acidic conditions in which silicate dissolution has been observed to increase with decreasing pH.[27] Our cluster differs from that used by Xiao and Lasaga[51] because the surface Si atom is bound to three other Si atoms through three bridging oxygen atoms and because the Si atoms are terminated by OH groups rather than H only.

The use of OH versus H, used in many previous studies to terminate the cluster, is critical because O−O repulsion between the approaching molecule and the silicate cluster must be accounted for in the reaction scheme. The repulsion energy curve of two O atoms approaching each other will differ significantly from that of an O atom approaching an H atom. Second, the H-bond between the approaching molecule (or ion) and the silicate cluster will be qualitatively different if there are H atoms terminating the cluster as opposed to O−H groups. Third, the electronic structure of the Si atom changes significantly with substitution of H for OH.[61] These differences have significant effects on the calculated activation energy and the calculated reaction path.

Our model system also differs from that used by Xiao and Lasaga[51] and Pelmenschikov et al.[56] because it includes explicit solvation by H_2O molecules. Inclusion of the extra H_2O molecules is important in modeling the reaction with H_3O^+ or H_2O for two reasons. First, proton-transfer reactions can be mediated by solvating H_2O molecules.[62] Second, H-bonding between the approaching H_3O^+ or H_2O and surrounding H_2O molecules will affect how strongly the approaching species interacts with the O_{br} atom of the silicate cluster. If there are no competing H-bonds, bonding between the approaching molecule or ion and the silicate framework will be overestimated.

The cluster used in our study differs from those with constrained terminal atoms modeled by Pelmenschikov et al.[56] because it is entirely unconstrained. Our approach allows the surface to have significant atomic relaxation during dissolution while the approach of Pelmenschikov et al.[56] allowed for minimal surface relaxation. The unconstrained calculations will simulate more closely the gel-like layers that form on some silicates and glasses[63−66] during dissolution. With the relaxed approach, however, calculated activation energies will most likely underestimate the true activation barrier (i.e., produce a lower limit); in the highly constrained approach, the opposite is true. Another significant difference with Pelmenschikov et al.[56] is that we calculated a reaction pathway to estimate a transition state structure instead of assuming a structure for the activated complex.

Materials and Methods

Ab initio calculations were carried out using the program Gaussian 98.[67] Structures for the Q^3Si cluster and steps along a hydrolysis reaction path were optimized using internal redundant coordinates[68] with the B3LYP/6-31G(d) method.[69−72] B3LYP is a density functional theory method that combines the Becke[70] gradient-corrected exchange functional with the Lee−Yang−Parr gradient-corrected correlation functional.[71] Hence, B3LYP/6-31G(d) is a hybrid molecular orbital-density functional theory method that provides for reasonable accuracy and computational efficiency.[73] Single-point calculations were performed on the B3LYP/6-31G(d)-optimized structures with the B3LYP/6-311+G(d,p) method (i.e., B3LYP/6-311+G(d,p)//B3LYP/6-31G(d)) to obtain more accurate energies.

A reaction path for the hydrolysis of Q^3Si was calculated by the method of constrained optimization.[74] We began with the fully optimized structure of the Q^3Si cluster with H-bonding between the hydronium ion and the bridging oxygen (O_{br}). In the forward direction, the hydronium ion was gradually moved stepwise toward the bridging oxygen in small increments (e.g., 0.1 Å) until a H^+ separated from H_3O^+ and protonated the bridging oxygen ($O_{br}H$). Then, the remaining H_2O was moved stepwise toward the Q^3Si until a pentacoordinate Si atom formed ($^{[5]}Si$). Portions of the reaction path were refined by calculating the reaction path in the reverse direction. This can be an important method in systems where multiple local minima are possible. In this case, H-bonding among the numerous OH groups present that would not exist in a periodic crystal structure can complicate the task of finding the lowest potential energy. In regions where more detail was required (e.g., near transition states), the reaction path was calculated by imposing constrained increments of 0.01 Å per step.

Vibrational frequencies were calculated with the B3LYP/6-31G(d) method to confirm attainment of local energy minima and transition state configurations along the reaction path and to calculate zero-point energies (ZPE). The Hessian (the second

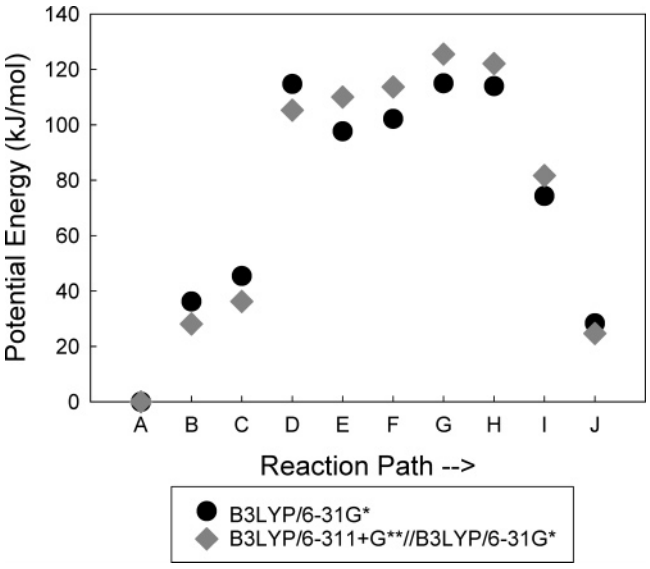

Figure 3. Calculated energies along the reaction path for Q^3Si hydrolysis at the B3LYP/6-31G(d) and B3LYP/6-311+G(d,p)//B3LYP/6-31G(d) levels of theory.

derivative matrix of the potential energy with respect to atomic coordinates) for an equilibrium configuration has positive eigenvalues for the potential energy with respect to atomic coordinates. In contrast, the Hessian for a transition state has one and only one negative eigenvalue that results in an imaginary frequency. The ZPE correction accounts for the effects of molecular vibrations that persist at 0 K and can be significant in calculating activation energies.[75] Because of systematic errors in the frequency calculations, the ZPEs need to be corrected by a scale factor of 0.9804, prior to addition to the energy of the optimized cluster geometry to obtain the total energy for the system.[76,77]

Results

The silicate hydrolysis reaction path is described in Figures 3 and 4. Figure 3 represents the changes in the energy along the reaction path, and Figure 4 illustrates configurations of the cluster along the reaction path. Three elementary steps have been hypothesized for silicate hydrolysis in an acidic environment:[51,78] (1) the protonation of a bridging oxygen atom (Figure 4B,C), (2) formation of a 5-coordinate Si intermediate (Figure 4D,E), and (3) the cleavage of a $Si-O_{br}$ bond (Figure 4F−H). From constrained geometry optimizations using B3LYP/6−31-(d), the protonation step is described by the following reactions:

$$Si_4O_3(OH)_{10}\cdots H_3O^+ + 4H_2O \leftrightarrow Si_4O_3(OH)_{10}(H_3O^+) + 4H_2O \quad (3)$$

$$Si_4O_3(OH)_{10}(H_3O^+) + 4H_2O \leftrightarrow Si_4O_2(OH)_{11}{}^+ + 5H_2O \quad (4)$$

In the initial configuration illustrated in Figure 4A, the hydronium ion is H-bonded to the framework silicate cluster. As this ion approaches a bridging oxygen atom, the hydronium ion forms a stronger bond with the silicate framework (Figure 4B). Upon further approach, a proton leaves the hydronium ion, creating a protonated bridging oxygen atom ($O_{br}H$) on the silicate surface and releasing a water molecule (Figure 4C,D). As this reaction progresses, the $Si-O_{br}$ bond lengths simultaneously increased from 1.65 and 1.69 Å to 1.79 and 1.78 Å, respectively, as has been predicted previously,[51,56,78] making the eventual hydrolysis of the SiOSi linkage easier. The configurations illustrated in Figures 4B−D all have one and only one imaginary frequency (unscaled values of −805, −728, and −85 cm^{-1}, respectively). Furthermore, the modes associated with these imaginary frequencies are consistent with the calculated reaction path, suggesting that these configurations represent a close approximation to the minimum energy reaction path.

The second and third steps in silicate hydrolysis, formation of a 5-coordinate intermediate and $Si-O_{br}$ cleavage, can be described by the following reactions:

$$Si_4O_2(OH)_{11}{}^+ + 5\,H_2O \leftrightarrow Si_4O_2(OH)_{11}{}^+\cdots H_2O + 4\,H_2O \quad (5)$$

$$Si_4O_2(OH)_{11}{}^+\cdots H_2O + 4H_2O \leftrightarrow Si_4O_2(OH)_{11}(H_2O)^+ + 4H_2O \quad (6)$$

$$Si_4O_2(OH)_{11}(H_2O)^+ + 4H_2O \leftrightarrow Si(OH)_4 + Si_3O_2(OH)_8 + 3H_2O + H_3O^+ \quad (7)$$

These steps are illustrated in Figure 4D−J. The water molecule that was initially part of the hydronium ion was progressively constrained to approach the Q^3Si atom in the cluster by fixing the $(H_2O)\cdots Si$ distance. Figure 4D illustrates the transition state to a stable intermediate with a 5-coordinate Si (Figure 4E) as predicted in Xiao and Lasaga.[51] In terms of the energy changes associated with silicate hydrolysis that are depicted in Figure 3, this is the first point along the reaction path calculated using B3LYP/6-31G(d) that clearly illustrates that an activation energy barrier has been passed (i.e., step #5 in Figure 3). Without the ZPE correction, this barrier is 112 kJ/mol. Including the ZPE correction, the estimated energy barrier to formation of the $^{[5]}Si$ species from the Q^3 SiOH molecule is 98 kJ/mol.

Upon formation of this metastable pentacoordinate Si configuration, the constrained parameter was switched to the $^{[5]}Si-O_{br}H$ distance. Because this bond is already lengthened by approximately 0.2 Å relative to the reactant structure (Figure 4A vs Figure 4E), increasing this distance in steps from 1.84 to 2.00, 2.20, 2.40, and 3.00 Å increased the overall potential energy by less than 20 kJ/mol (Figure 3). The local potential energy maximum for breaking the $^{[5]}Si-O_{br}H$ bond occurs at a distance of 2.40 Å (Figure 4H). We conclude that the rate-limiting step in the hydrolysis of Si−O−Si linkages in silica is the formation of the pentacoordinate Si configuration as suggested previously[51] because the formation of the $^{[5]}Si$ requires the greatest component of energy in the overall reaction path.

Note that a proton from the attacking H_2O molecule transfers to one of the solvating H_2O molecules soon after hydrolysis occurs (Figure 4I−J), but this proton transfer starts to occur as soon as the 5-fold Si is formed (Figure 4E), as indicated by a decreasing distance between the $Si-(OH_2)^+$ group and the H_2O molecule involved in the reaction. That H^+ transfer back to a solvating H_2O molecule plays a role in the hydrolysis mechanism illustrates the importance of including explicit solvation in these models to describe silicate hydrolysis. Although more H_2O molecules might improve the simulation, without this minimal number of H_2O molecules solvating part of the silicate cluster, this type of H^+ transfer could not take place.

Selected points along the reaction pathway (e.g., near potential energy maxima) illustrated in Figures 3 and 4 were subjected to frequency analysis. The configuration of the local potential energy maxima all resulted in one and only one imaginary

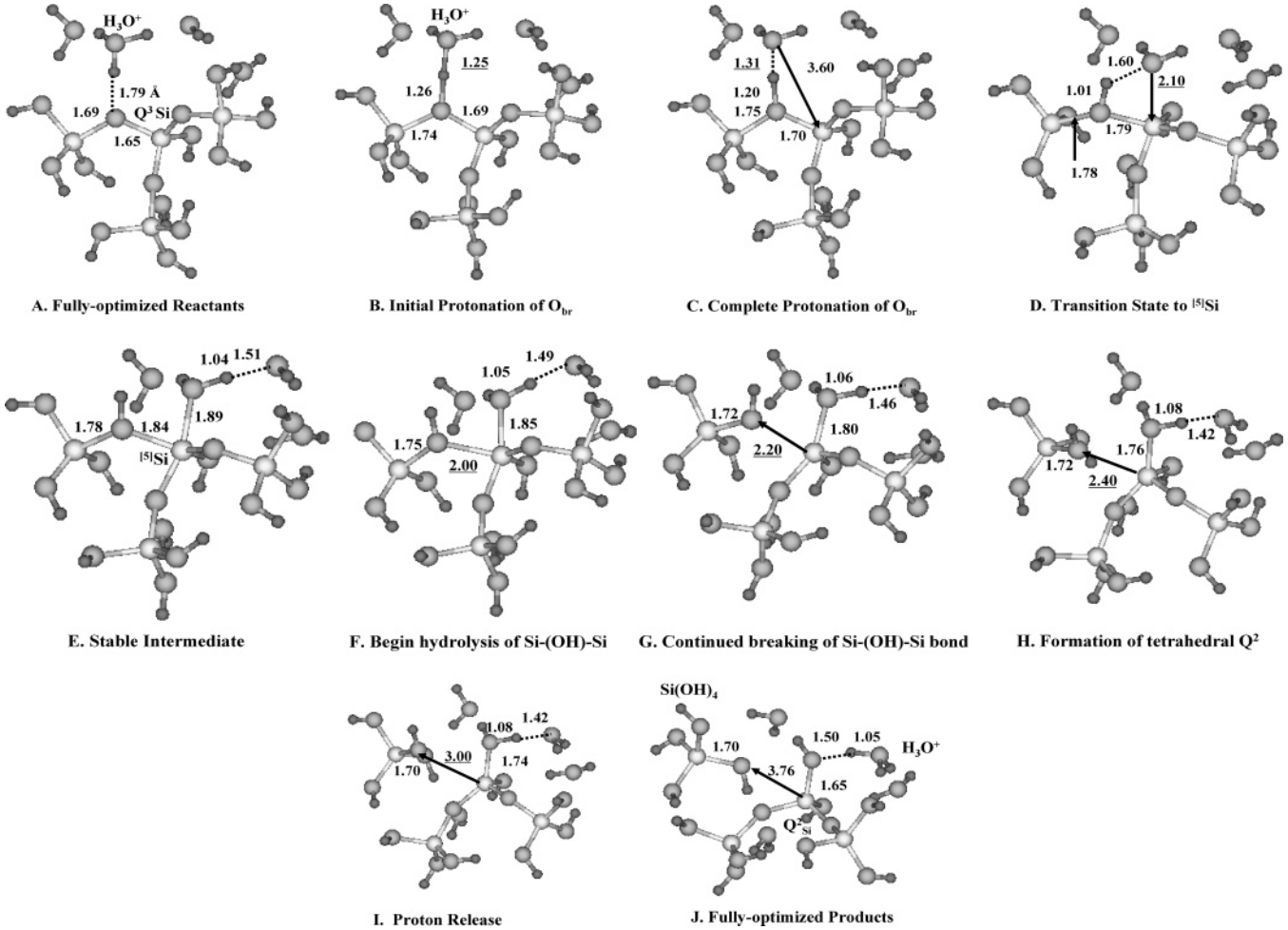

Figure 4. Geometries of the hydrous silicate cluster along the reaction path calculated using B3LYP/6-31G(d): (A) fully optimized reactants, (B) initial protonation of bridging oxygen, (C) complete protonation of bridging oxygen, (D) transition state to 5-fold silicon, (E) stable 5-fold intermediate, (F) hydrolysis of the $^{[5]}Si-O_{br}H-Si$ begins, (G) $^{[5]}Si-O_{br}H$ constrained to 2.2 Å, (H) $^{[5]}Si-O_{br}H$ constrained to 2.4 Å, (I) $^{[5]}Si-O_{br}H$ constrained to 3.0 Å, and (J) fully optimized products. The underscored distances in panels B−D and E−I indicate the constraint used in the optimization presented. The B3LYP/6-31G(d) configurations in panels B−C are taken from the backwards reaction path in which the bridging oxygen is deprotonated to form the hydronium ion. Figure 4H illustrates the configuration for the highest energy point calculated along the reaction path using B3LYP/6-31G(d).

frequency. The vibrational modes of these imaginary frequencies are illustrated in Figure 5. Because these configurations represent local maxima, have only one imaginary frequency, and the displacements of these imaginary modes point toward the next step calculated along the reaction pathway, they are reasonable approximations to transition states.[79] Further refinement could result in modified structures closer to the true transition states, but for our purposes, these approximations are sufficient.

Discussion

Previous work suggested that dissolution of silica could occur via an H^+-catalyzed mechanism.[51] A key factor in evaluating whether the protonation of bridging oxygen atoms can catalyze silica dissolution is the relative heights of the energy barriers associated with protonation and hydrolysis of the $Si-O_{br}$ bond. Xiao and Lasaga[51] predicted that proton adsorption on a bridging oxygen would have a favorable adsorption enthalpy of −16 kJ/mol. However, spectroscopic studies, such as IR and NMR,[80,81] do not reveal features suggestive of Si−(OH)−Si linkages. Furthermore, when Si−(OH)−Si linkages are present in siliceous zeolites, these sites are highly acidic.[82,83]

Because of the approximations made in the earlier ab initio study of Xiao and Lasaga,[51] we hypothesized that H^+ adsorption onto O_{br} atoms in silica would be energetically favorable. However, our calculations predict that this protonation requires 45 kJ/mol; therefore, Si−(OH)−Si species should occur only in trace quantities on a silica surface. This calculated value for protonating the bridging oxygen is significantly lower, however, than the experimental activation energies of silica dissolution that are in the range of 60−95 kJ/mol.[84] We conclude that the protonation of a bridging oxygen has a large enough energy barrier that it will not form a major surface species detectable via spectroscopic techniques under normal pH conditions (pH > 2) but that the energy barrier is small enough to allow formation of a trace concentration of these species that can play a role in the dissolution reaction. Formation of a trace concentration of protonated bridging oxygen atoms on a silica surface is consistent with the deductions of Dove[85] based on a detailed macroscopic investigation of quartz dissolution rates.

The activation energy, ΔE_a, calculated here for hydrolysis of an unconstrained Q^3 Si $-O_{br}$ bond, is between ∼115 kJ/mol (B3LYP/6-31G(d)) and ∼125 kJ/mol (B3LYP/6-31G(d)//B3LYP/6-311+G(d,p)) and lies between activation energies calculated by Pelmenschikov et al.[56,57] for hydrolysis of constrained geometries of Q^2Si-O_{br} and Q^3Si-O_{br} (Table 2) by H_2O in a vacuum. If the Pelmenschikov et al.[56] approach overestimates the activation energy of hydrolysis because of the assumption of minimal relaxation of the molecular geometry at the mineral

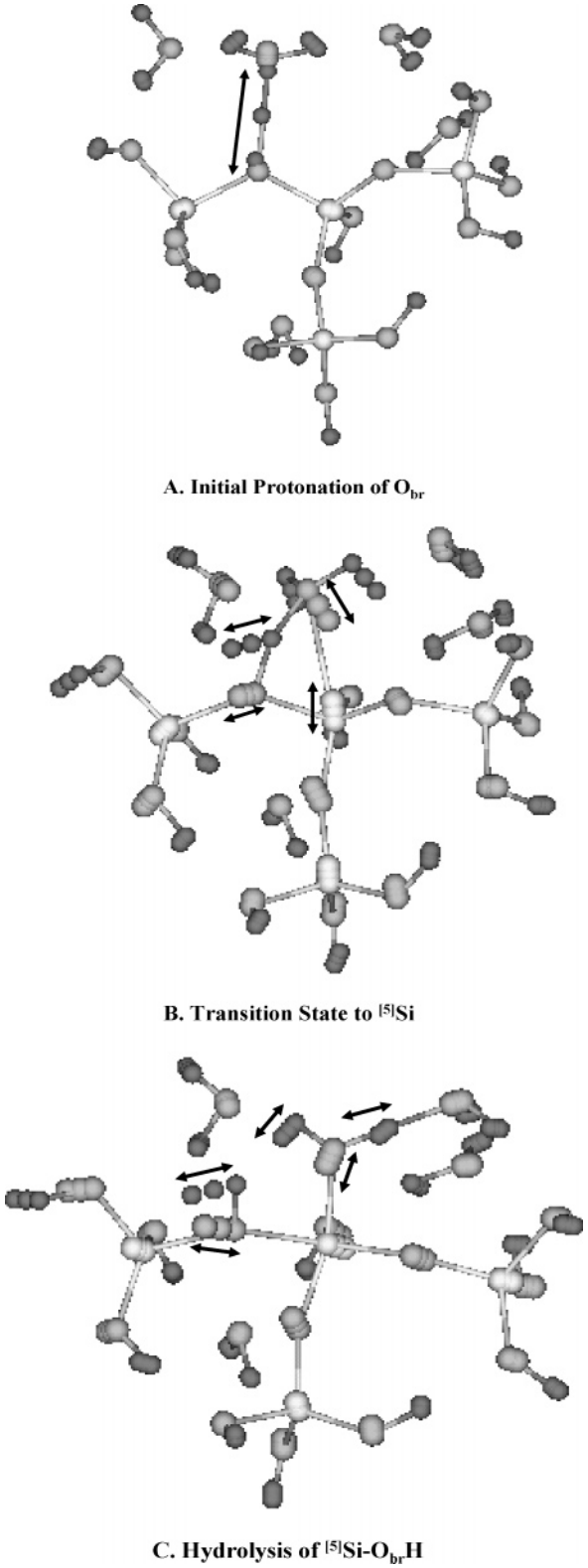

Figure 5. Displacements of the imaginary modes associated with each of the approximate transition states (A) to protonating the bridging oxygen atom, (B) to the pentacoordinate Si, and (C) hydrolysis of the $^{[5]}Si-O_{br}H-Si$ linkage. These figures correspond to Figure 4B,D,H, respectively, along the reaction path. Arrows are included as guides to the important molecular displacements along the reaction pathway. Each figure represents the only imaginary frequency calculated for this configuration.

surface, then we can conclude that the activation energy for hydrolysis of Q^3Si-O_{br} at a mineral surface is most likely between 120 kJ/mol (an average of our calculated values, without the ZPE correction) and 138 kJ/mol (result of Pelmenschikov et al.[56]). Given that the experimental activation energy for silica dissolution has been measured to lie within a range with a maximum of about 90 kJ/mol (Table 2), both our calculated values and that of Pelmenschikov et al.[56] significantly overestimate the observed value.

Pelmenschikov et al.[57] also found that calculated activation energies increased by approximately 15 kJ/mol when implicit solvation is considered. Our model takes into account partial explicit solvation of the cluster. In bulk solution, a hydronium ion is solvated by two[86] or three[87] water molecules and has an associated solvation energy of −1071[86] or −1098[87] kJ/mol. Our model does not take into account the difference in energy required to replace a H-bond between the hydronium ion and a water molecule with a H-bond between the hydronium ion and the silicate framework. It does include the energy of solvation between the hydronium ion and two water molecules as well as the energy of solvation for the Si−OH representing the silica surface. The inclusion of explicit solvation in our calculations increases our calculated activation energy for hydrolysis, hence increasing the discrepancy with observation.

There are a number of additional model-dependent reasons why our calculations might result in an activation energy higher than that observed experimentally including the use of a limited basis set and the incomplete treatment of electron correlation. However, using the B3LYP level of theory and several different basis sets, Felipe et al.[62] calculated the zero-point energy corrected barriers (ZPECB) for the exchange of a hydrogen atom from one of three water molecules to a molecule of orthosilicic acid (H_4SiO_4). They found no apparent trend in computed ZPECB with the level of a chosen basis set. Felipe et al.[62] also calculated the reaction pathway using MP2/6-31+G(d,p). The ZPECB calculated at the MP2 level was almost twice as large as that calculated at the B3LYP level. Furthermore, the direction of the equilibrium was opposite to that of both the B3LYP calculations and the experimental data. These results suggest that it is very uncertain whether higher level calculations would provide more reliable values for the activation energy barrier associated with $Si-O_{br}$ hydrolysis than those (i.e., B3LYP/6-31G(d,p)) presented here.

Our activation energy barrier should be lower by approximately 20−60 kJ/mol as compared to the case where lattice constraints are imposed[57] due to the full relaxation of surrounding atoms allowed in our calculations. However, the presence of explicit water molecules in our cluster should increase the predicted energy barrier, explaining, in part, why our calculated activation energy is higher than that reported in Xiao and Lasaga.[51] Calculations that include both explicit water molecules and implicit long-range effects tend to increase calculated activation energy barriers at temperatures below 1000 K.[62] On the basis of all these considerations, it is safe to conclude that our results in combination with those of Pelmenschikov et al.[56,57] successfully bracket the activation energy associated with breaking a Q^3Si-O_{br} bond. Our calculations should best predict reactions on a gel-like surface such as those hypothesized on acid-etched feldspars.

This result suggests that measured experimental activation energies do not correspond to the hydrolysis of a Q^3Si-O_{br} bond. This outcome is consistent with Pelmenschikov et al.,[57] who concluded that the measured dissolution rates for silica are related to the breakage of the last Si−O−Si bond (Q^1Si). Activation energies measured for silicates (Table 2) also do not show a trend as a function of connectedness. Most of the measured activation energies for pyroxenes (connectedness =

TABLE 1: Calculated Potential Energies (hartrees) for the Structures Illustrated in Figure 4

Configuration	constraint (Å)	B3LYP/6-31G(d)	B3LYP/631G(d,p)//B3LYP/6-31G(d)	ZPE
A	none	−2525.2373	−2525.9404	0.3048
B	1.25	−2525.2194	−2525.9256	0.3006
C	1.31	−2525.2159	−2525.9225	0.3006[a]
D	1.60	−2525.1948	−2525.9015	0.3060[a]
E	none	−2525.2025	−2525.9009	0.3072
F	2.00	−2525.1996	−2525.8983	*b*
G	2.20	−2525.1947	−2525.8938	*b*
H	2.40	−2525.1936	−2525.8936	0.3045[a]
I	3.00	−2525.2090	−2525.9105	*b*
J	none	−2525.2255	−2525.9300	0.3038

[a] Indicates transition state. [b] The blank cells under ZPE indicate no frequency calculation, and none is needed because this is not a stationary point.

TABLE 2: Calculated and Measured Activation Energies (kJ/mol)

phase or cluster	calculated	measured	connectedness[a]	ref
unconstrained, $Q^1Si\text{-}O_{br}$	100		1	51
unconstrained, $Q^1Si\text{-}O_{br}$	71		1	56 and 57
β-cristobalite, $Q^2Si\text{-}O\text{-}Q^4Si$	92		2	56 and 57
β-cristobalite, $Q^3Si\text{-}O\text{-}Q^4Si$	138		3	56 and 57
β-cristobalite, $Q^4Si\text{-}O\text{-}Q^4Si$	205		4	56 and 57
Unconstrained $Q^3Si\text{-}O\text{-}Q^1Si$	112		3	this paper
Quartz		67−88	4	53, 55, 88, 89
albite feldspar		59−67	3	90 and 91
Anorthite		79	0	90
Kaolinite		54−67	3	92 and 93
Anthophyllite		79	2.5	23
Enstatite		50	2	17
Diopside		46−96	2	15 and 23
Forsterite		42−126	0	11 and 12

[a] Number of bridging oxygens around the Si atom involved in the inferred rate-limiting step during acid dissolution. Note that for feldspars, Al is leached at low pH, and the inferred connectedness of the precursor to dissolution has a lower connectedness than Si in bulk feldspars.

2), amphiboles (2.5), phyllosilicates (3), alkali feldspars (3, after leaching of Al), and quartz (4) suggest that the connectedness of the Si atom involved in the rate-limiting step is 2 or less (Figure 6). Earlier studies[94] have suggested that Q^2 sites (i.e., edge sites) may be the focus of hydrolysis on the surface for silicates and aluminosilicates. Further studies using our approach for Q^3 Si to examine the hydrolysis of Q^2 Si and Q^1 Si should exhibit a decrease in activation energy with decreasing Si connectedness, analogous to that observed by Pelmenshikov et al.[56] If we assume that our calculated activation energies for the hydrolysis of an Si−O bond would decrease in the following order $Q^3Si > Q^2Si > Q^1Si$, approximately the same magnitude as those calculated by Pelmenshikov et al.,[56] then our activation energy for the hydrolysis of Q^2 Si would be approximately 74 kJ/mol. This calculated activation energy fits very nicely within the range of measured activation energies for the dissolution of silicate minerals shown in Figure 6. In addition, the measured activation energy of Gratz et al.[33] for a face of quartz dominated by Q^3 (the major rhombohedral face, 90.19 kJ/ mol) as compared to a face composed of Q^2 and Q^3 (the prism face of quartz, 86.39 kJ/mol), is again consistent with hydrolysis of Q^2 as the rate-limiting step and with the activation energy for this step lying between our estimate for Q^2 (74 kJ/mol) and the estimate for Q^3 (120 kJ/mol).

Although the reaction path presented here may not be the rate-limiting path for silicate dissolution because we used a Q^3-Si model, the concerted mechanism described here, involving proton transfer, formation of a $^{[5]}Si$, and hydrolysis of a $^{[5]}Si-(OH)-Si$ linkage is likely to include the elementary steps in silicate dissolution regardless of the Q number. Even if the agent of dissolution is H_2O instead of H_3O^+, most theoretical studies suggest the formation of a $^{[5]}Si-(OH_2)^+$ surface complex. Thus, an H^+ must transfer from this surface group to allow formation of the next lower polymerization state (i.e., Q^3 to Q^2, Q^2 to Q^1, or Q^1 to Q^0). Consequently, inclusion of explicit solvation in addition to any implicit solvation methods is required to map out an appropriate reaction pathway on the potential energy

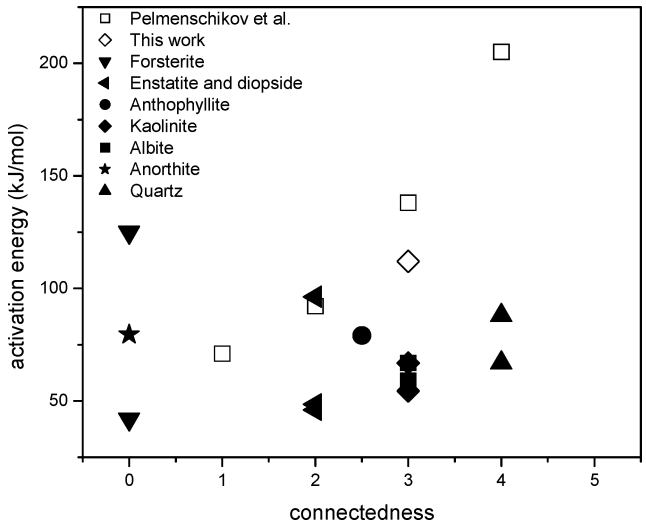

Figure 6. Estimates of the pH-independent activation energy for dissolution at low pH for selected minerals plotted vs connectedness for the dissolving phase. Original sources for experimental data are summarized in Brantley.[27] For quartz, forsterite, diopside, albite, and kaolinite, the highest and lowest reported values of activation energies are plotted (i.e., the range of reported values), based on data in Table 6 of Brantley.[27] Estimates of activation energy calculated by Pelmenshickov et al.[56,57] and based on this work calculated using B3LYP/6-31(d) are also included. Connectedness of anorthite is assumed during dissolution to equal 0 because Al is leached first, leaving Si tetrahedra without bridging oxygens. Similarly, albite is plotted assuming a connectedness of 3.

surface. Furthermore, the reaction pathway must be mapped out in detail to estimate the transition-state complex configuration and activation energy. Any assumptions about the structure of the transition-state complex (e.g., Pelmenschikov et al.[56]) are likely to be oversimplified as compared to the configuration determined by following the reaction path.

Conclusions

In this investigation, we represent the silicate surfaces by large clusters and include four water molecules to partially account for explicit solvation. We use fully relaxed clusters, OH rather than H to terminate our silicate molecules, and calculate full reaction paths. Because we included two water molecules that are H-bonded to the hydronium ion, our calculations predict that the protonation of an O_{br} atom requires 45 kJ/mol, so that the Si−(OH)−Si species should only occur in trace quantities on a silica surface. This result differs from that of Xiao and Lasaga who found that the adsorption of H^+ onto O_{br} atoms would be energetically favorable (−16 kJ/mol). Like the results of Pelmenschikov et al.,[56] our calculations suggest that including the effects of solvation increases the calculated activation energy of $Si-O_{br}$ hydrolysis. Our calculations demonstrate that proton transfer from the attacking H_2O to one of the solvating H_2O molecules starts to occur as soon as 5-fold Si is formed, thus playing a role in the hydrolysis mechanism. This reaction would go unnoticed without explicit H_2O molecules in the model cluster. Finally, by comparing our calculated activation energies with both measured experimental and calculated[56,57] activation energies, we can conclude that measured activation energies for the hydrolysis of silicate minerals are most consistent with hydrolysis of Q^2Si-O_{br} bonds and that the breaking of these bonds represents the rate-limiting step during dissolution.

Acknowledgment. Review comments from P. M. Dove, J. A. Greathouse, S. L. Rempe, and two anonymous reviewers are greatly appreciated. J.D.K. acknowledges the support of the Office of Naval Research, the National Science Foundation (EAR-0073722), and the U. S. Department of Energy Office of Basic Energy Sciences, Division of Chemical Sciences, Geosciences and Biosciences, under the Project "Nanoscale Complexity at the Oxide-Water Interface". In addition, computational support was provided by the High-Performance Computing Modernization Office of the Department of Defense. S.L.B. acknowledges support from DOE Grant DE-FG02-01ER15209 from the Office of Basic Energy Sciences. L.J.C. was funded by these grants while at the Pennsylvania State University (2000−2001). She acknowledges current support from the U.S. Department of Energy, Office of Basic Energy Sciences, Division of Chemical Sciences, Geosciences, and Biosciences. Sandia is a multiprogram laboratory operated by Sandia Corporation, a Lockheed Martin company, for the U.S. Department of Energy under Contract DE-AC04-94AL85000.

References and Notes

(1) White, A. F.; Brantley, S. L. *Chemical Weathering Rates of Silicate Minerals, Reviews in Mineralogy 31*; Mineralogical Society of America: Washington, DC, 1995.

(2) Bunker, B. C.; Tallant, D. R.; Headley, T. J.; Turner, G. L.; Kirkpatrick, R. J. *Phys. Chem. Glasses* **1988**, *29*, 106.

(3) Kirkpatrick, R. J. *Spectroscopic Methods in Mineralogy and Geology, Reviews in Mineralogy 18*; Hawthorne, F. C., Ed; Mineralogical Society of America: Washington, DC, 1988; pp 341−404.

(4) Liebau, F. *Structural Chemistry of Silicates*; Springer-Verlag: Berlin, 1985.

(5) Swaddle, T. W. *Coord. Chem. Rev.* **2001**, *219*−*221*, 665.

(6) Harris, R. K.; Knight, C. T. G. *J. Mol. Struct.* **1982**, *78*, 273.

(7) Harris, R. K.; Knight, C. T. G. *J. Chem. Soc., Faraday Trans. 2* **1983**, *79*, 1525.

(8) Harris, R. K.; Knight, C. T. G. *J. Chem. Soc., Faraday Trans. 2* **1983**, *79*, 1539.

(9) Kinrade, S. D.; Swaddle, T. W. *Inorg. Chem.* **1988**, *27*, 4253.

(10) Harris, R. K.; Bahlmann, E. K. F.; Metcalfe, K.; Smith, E. G. *Magn. Reson. Chem.* **1999**, *31*, 743.

(11) Chen, Y.; Brantley, S. L. *Chem. Geol.* **2000**, *165*, 267.

(12) Rosso, J. J.; Rimstidt, J. D. *Geochim. Cosmochim. Acta* **2000**, *64*, 797.

(13) Westrich, H. R.; Cygan, R. T.; Casey, W. H.; Zemitis, C.; Arbold, G. W. *Am. J. Sci.* **1993**, *293*, 869.

(14) Casey, W. H.; Hochella, M. F., Jr.; Westrich, H. R. *Geochim. Cosmochim. Acta* **1993**, *57*, 785.

(15) Knauss, K. G.; Nguyen, S. N.; Weed, H. C. *Geochim. Cosmochim. Acta* **1993**, *57*, 285.

(16) Feruzzi, G. G. The character and rates of dissolution of pyroxenes and pyroxenoids, MS Thesis, University of California, Davis, CA, 1993.

(17) Oelkers, E. H.; Schott, J. *Geochim. Cosmochim. Acta* **2001**, *65*, 1219.

(18) Xie, Z. Surface properties of silicates, their solubility, and dissolution kinetics. Ph.D. Thesis, Northwestern University, Evanston, IL, 1994.

(19) Weissbart, E. J.; Rimstidt, J. D. *Geochim. Cosmochim. Acta* **2000**, *64*, 4007.

(20) Banfield, J. F.; Ferruzzi, C. G.; Casey, W. H.; Westrich, H. R. *Geochim. Cosmochim. Acta* **1995**, *59*, 19.

(21) Siegel, D. I.; Pfannkuch, H. O. *Geochim. Cosmochim. Acta* **1984**, *48*, 197.

(22) Sverdrup, H. U. *The Kinetics of Base Cation Release Due to Chemical Weatherin*g; Lund University Press: Lund, Sweden, 1990.

(23) Chen, Y.; Brantley, S. L. *Chem. Geol.* **1998**, *147*, 233.

(24) Mast, M. A.; Drever, J. I. *Geochim. Cosmochim. Acta* **1987**, *51*, 2559.

(25) Schott, J.; Berner, R. A.; Sjoberg, E. L. *Geochim. Cosmochim. Acta* **1981**, *45*, 2123.

(26) Frogner, P.; Schweda, P. *Chem. Geol.* **1998**, *151*, 169.

(27) Brantley, S. L. *Surface and Groundwater, Weathering, and Soils*; Drever, J. I., Ed; Elsevier: Amsterdam, 2004; Vol. 5, pp 73−117.

(28) Brantley, S. L.; Chen, Y. *Chemical Weathering Rates of Silicate Mineral, Reviews in Mineralogy 31*; White, A. F., Brantley, S. L., Eds; Mineralogical Society of America: Washington, DC, 1995; pp 119−172.

(29) Casey, W. H.; Westrich, H. R. *Nature* **1992**, *355*, 157.

(30) Geisinger, K. L.; Gibbs, G. V.; Navrotsky, A. *Phys. Chem. Miner.* **1985**, *11*, 266−283.

(31) Navrotsky, A.; Geisinger, K. L.; McMillan, P.; Gibbs, G. V. *Phys. Chem. Min.* **1985**, *11*, 284.

(32) Gratz, A. J.; Bird, P. *Geochim. Cosmochim. Acta* **1993**, *57*, 965.

(33) Gratz, A. J.; Bird, P. *Geochim. Cosmochim. Acta* **1993**, *57*, 977.

(34) Blum, A. E.; Lasaga, A. C. *Nature* **1988**, *331*, 431.

(35) Blum, A. E.; Lasaga, A. C. *Geochim. Cosmochim. Acta* **1991**, *55*, 2193.

(36) Busenberg, E.; Clemency, C. V. *Geochim. Cosmochim. Acta* **1976**, *40*, 41.

(37) Casey, W. H.; Westrich, H. R.; Holdren, G. R. *Am. Mineral.* **1991**, *76*, 211.

(38) Chou, L.; Wollast, R. *Am. J. Sci.* **1984**, *285*, 963.

(39) Holdren, G. R.; Berner, R. A. *Geochim. Cosmochim. Acta* **1979**, *43*, 1161.

(40) Holdren, G. R.; Speyer, P. M. *Geochim. Cosmochim. Acta* **1987**, *51*, 2311.

(41) Rose, N. M. *Geochim. Cosmochim. Acta* **1991**, *55*, 3273.

(42) Schewda, P. Proceedings of the 6th International Symposium of Water Rock Interaction; Miles, D. L., Ed.; A. A. Balkema: Brookfield, VT, 1989; pp 609−612.

(43) Stillings, L. L.; Brantley, S. L. *Geochim. Cosmochim. Acta* **1995**, *59*, 1483.

(44) Stillings, L. L.; Drever, J. L.; Brantley, S. L.; Sun, Y.; Oxburgh, R. *Chem. Geol.* **1996**, *132*, 79.

(45) Brady, P. V.; Walther, J. V. *Chem. Geol.* **1990**, *82*, 253.

(46) Brady, P. V.; Walther, J. V. *Am. J. Sci.* **1992**, *292*, 639.

(47) Feuston, B. P.; Garofalini, S. H. *J. Appl. Phys.* **1990**, *68*, 4830.

(48) Ferrari, A. M.; Garrone, E.; Spoto, G.; Ugliengo, P.; Zecchina, A. *Surf. Sci.* **1995**, *323*, 151.

(49) Walsh, T. R.; Wilson, M.; Sutton, A. P. *J. Chem. Phys.* **2000**, *113*, 9191.

(50) Masini, P.; Bernasconi, M. *J. Phys.: Condensed Matter* **2002**, *14*, 4133.

(51) Xiao, Y.; Lasaga, A. C. *Geochem. Cosmochim. Acta* **1994**, *58*, 5379.

(52) Yamabe, S.; Minato, T.; Hirao, K. *J. Chem. Phys.* **1984**, *80*, 1576.

(53) Rimstidt, J. D.; Barnes, H. L. *Geochim. Cosmochim. Acta* **1980**, *44*, 1683.

(54) Mazer, J. J.; Walther, J. V. *J. Non-Cryst. Solids* **1994**, *170*, 32.

(55) Tester, J. W.; Worley, W. G.; Robinson, B. A.; Grigsby, C. O.; Feerer, J. L. *Geochim. Cosmochim. Acta* **1994**, *58*, 2407.
(56) Pelmenschikov, A.; Strandh, H.; Pettersson, L. G. M.; Leszcyzynski, J. *J. Phys. Chem. B* **2000**, *104*, 5779.
(57) Pelmenschikov, A.; Leszczynski, J.; Pettersson, L. G. M. *J. Phys. Chem. A* **2001**, *105*, 9528.
(58) Knauss, K. G.; Wolery, T. J. *Geochim. Cosmochim. Acta* **1988**, *53*, 1493.
(59) Dove, P. M.; Crerar, D. A. *Geochim. Cosmochim. Acta* **1990**, *54*, 955.
(60) Walther, J. V. *Am. J. Sci.* **1996**, *296*, 693.
(61) Tossell, J. A.; Sághi-Szabó, G. *Geochim. Cosmochim. Acta* **1997**, *61*, 1171.
(62) Felipe, M. A.; Kubicki, J. D.; Rye, D. M. *Geochim. Cosmochim. Acta* **2003**, *67*, 1259.
(63) Casey, W. H.; Westrich, H. R.; Arnold, G. W.; Banfield, J. F. *Geochim. Cosmochim. Acta* **1989**, *53*, 821.
(64) Hamilton, J. P.; Brantley, S. L.; Pantano, C. G.; Criscenti, L. J.; Kubicki, J. D. *Geochim. Cosmochim. Acta* **2001**, *65*, 3683.
(65) Hamilton, J. P.; Pantano, C. G.; Brantley, S. L. *Geochim. Cosmochim. Acta* **2000**, *64*, 2603.
(66) Hellmann, R. *Geochim. Cosmochim. Acta* **1997**, *61*, 1595.
(67) Frisch, M. J.; Trucks, G. W.; Schlegel, H. B.; Scuseria, G. E.; Robb, M. A.; Cheeseman, J. R.; Zakrzewski, V. G.; Montgomery, J. A.; Stratmann, R. E.; Burant, J. C.; Dapprich, S.; Millam, J. M.; Daniels, A. D.; Kudin, K. N.; Strain, M. C.; Farkas, O.; Tomasi, J.; Barone, V.; Cossi, M.; Cammi, R.; Mennucci, B.; Pomelli, C.; Adamo, C.; Clifford, S.; Ochterski, J.; Petersson, G. A.; Ayala, P. Y.; Cui, Q.; Morokuma, K.; Malick, D. K.; Rabuck, A. D.; Raghavachari, K.; Foresman, J. B.; Cioslowski, J.; Oritz, J. V.; Stefanov, B.; Liu, G.; Liashenko, A.; Piskorz, P.; Komaromi, I.; Gomperts, R.; Martin, R. L.; Fox, D. J.; Keith, T.; Al-Laham, M. A.; Peng, C. Y.; Nanayakkara, A.; Gonzalez, C.; Challacombe, M.; Gill, P. M. W.; Johnson, B. G.; Chen, W.; Wong, M. W.; Andres, J. L.; Head-Gordon, M.; Replogle, E. S.; Pople, J. A. *Gaussian 98* Gaussian, Inc.: Pittsburgh, 1998.
(68) Peng, C.; Ayala, P. Y.; Schlegel, H. B. *J. Comput. Chem.* **1996**, *17*, 49.
(69) Binkley, J. S.; Pople, J. A.; Hehre, W. J. *J. Am. Chem. Soc.* **1980**, *102*, 939.
(70) Becke, A. D. *Phys. Rev. A* **1988**, *38*, 3098.
(71) Lee, C.; Yang, W.; Parr, R. G. *Phys. Rev. B* **1988**, *37*, 785.
(72) Gordon, M. S.; Binkley, S.; Pople, J. A.; Pietro, W. J.; Hehre, W. J. *J. Am. Chem. Soc.* **1982**, *104*, 2797.
(73) Hehre, W. J.; Radom, L.; Schleyer, P. R.; Pople J. A. *Ab Initio Molecular Orbital Theory;* Wiley-Interscience: New York, 1986.
(74) Felipe, M. A.; Xiao, Y.; Kubicki, J. D. *Molecular Modeling Theory: Applications in the Geosciences, Reviews in Mineralogy 42*; Cygan, R. T., Kubicki, J. D., Eds.; Geochemical Society and Mineralogical Society of America: Washington, DC, 2001; pp 485−531.
(75) Lasaga, A. C. *Kinetic Theory in the Earth Sciences*; Princeton University Press: Princeton, NJ, 1998.
(76) Foresman, J. B.; Frisch, A. *Exploring Chemistry with Electronic Structure Methods*; Gaussian, Inc.: Pittsburgh, 1996.
(77) Scott, A. P.; Radom, L. *J. Phys. Chem.* **1996**, *100*, 16502.
(78) Casey, W. H.; Lasaga, A. C.; Gibbs, G. V. *Geochim. Cosmochim. Acta* **1990**, *54*, 3369.
(79) Cramer, C. J. *Essentials of Computational Chemistry*; John Wiley & Sons: West Sussex, England, 2002.
(80) Morrow, B. A.; Cody, I. A. *J. Phys. Chem.* **1973**, *77*, 1465.
(81) Carroll, S. A.; Maxwell, R. S.; Bourcier, W.; Martin, S.; Hulsey, S. *Geochim. Cosmochim. Acta* **2002**, *66*, 913.
(82) Nicholas, J. B.; Winans, R. E.; Harrison, R. J.; Iton, L. E.; Curtiss, L. A.; Hopfinger, A. J. *J. Phys. Chem.* **1992**, *96*, 10247.
(83) Kramer, G. J.; van Santen, R. A. *J. Am. Chem. Soc.* **1993**, *115*, 2887.
(84) Dove, P. M. *Chemical Weathering Rates of Silicate Minerals, Reviews in Mineralogy 31;* White, A. F., Brantley, S. L., Eds.; Mineralogical Society of America: Washington, DC, 1995; pp 235−290.
(85) Dove, P. M. *Am. J. Sci.* **1994**, *291*, 665.
(86) Grabowski, P.; Riccardi, D.; Gomez, M. A.; Asthagiri, D.; Pratt, L. R. *J. Phys. Chem. A* **2002**, *106*, 9148.
(87) Zhan, C.-G.; Dixon, D. A. *J. Phys. Chem. A* **2001**, *105*, 11534.
(88) Polster, W. Hydrothermal precipitation and dissolution of silica: Part I. Conditions in geothermal fields and sedimentary basins: Part II. Experimental evaluation of kinetics, Ph.D. Thesis, Pennsylvania State University, University Park, PA, 1994.
(89) Dove, P. M. *Geochim. Cosmochim. Acta* **1999**, *63*, 3715.
(90) Blum, A. E.; Stillings, L. L. *Chemical Weathering Rates of Silicate Minerals, Reviews in Mineralogy 31*; White, A. F.; Brantley, S. L., Eds; Mineralogical Society of America: Washington, DC, 1995; pp 291−352.
(91) Chen, Y.; Brantley, S. L. *Chem. Geol.* **1997**, *135*, 275.
(92) Kline, W. E.; Fogler, H. S. *Chem. Eng. Sci.* **1981**, *36*, 871.
(93) Carroll, S. A.; Walther, J. V. *Am. J. Sci.* **1991**, *290*, 797.
(94) Teng, H. H.; Fenter, P.; Cheng, L.; Sturchio, N. C. *Geochim. Cosmochim. Acta* **2001**, *65*, 3459.